ISSN No. 2455-5800
Journal of Scientific Research in Allied Sciences

Original Research Article

MATHEMATICAL MODELING AND SIMULATION TO PREDICT THE DEFORMATION RATE FROM HYDROCARBON IN CONCRETE PAVEMENTS

[1, 2] Eluozo. S. N and [2] Ode .T.
1. Subaka Nigeria Limited Port Harcourt Rivers State of Nigeria,
Director and Principal Consultant Civil and Environmental Engineering,
Research and Development
2. Department of Civil Engineering, faculty of Engineering, Rivers State University of Science and Technology Port Harcourt

Article history:
Submitted on: July 2016
Accepted on: August 2016
Email: info@jusres.com

ABSTRACT

The levels of concentration were monitored to determine the rate of hydrocarbon induced in concrete pavement. The study express the rate of concentration at different curing age, simulation values generated linear increase to the optimum values at various curing age, the rate of hydrocarbon increase can be attributed to high rate of porosity and permeability in the concrete formation. The behaviuor of the induced hydrocarbon are influenced by these parameters in the system. the developed model were simulated to predictive the deformation of hydrocarbon in concrete pavement, the system has express the rate of concentration at different curing age, comparism of both parameters developed faviourable fits, experts applying these concept will definitely observed various rate of induced hydrocarbon at various curing age in concrete pavement.

KEYWORDS: Mathematical Modeling, Hydrocarbon, and Concrete Pavement

1. INTRODUCTION

Contaminants in concrete may be salts (chlorides, sulphates, etc), silt, clay and hydrocarbon (petroleum product, etc). Generally, raw materials for concrete production should be free from contaminants. Laboratory test of concrete cubes cured in various hydrocarbon compounds was undertaken. The results indicated that petroleum hydrocarbons have no appreciative effect on concrete that has achieved its design strength, but it affects hardened concrete that has achieved its design strength (Wilson et al, 2001). The bearing capacity of reinforced concrete sections subjected to oil influence was found to decrease when compared with those of non-oiling influence (Blaszczynski and Scigallo, 2006). The effects of oil-based pollutants on the strength and integrity of building materials were examined. The physical testing programme indicated a positive effect with regard to compressive strength and slump of contaminated aggregate (Al-Mutairi, 1995) the presence of contaminants seems to interfere the cement-water binding reactions, delaying or preventing full hydration of cement particles (Calabrese et al, 1991Eluozo 2013b) the Presence of clay (contaminant) in a significant proportion in concrete reduces its compressive strength and increases its shrinkage value (Munoz et al, 2005). Incorporating marine clay and industrial sludge in concrete produced compressive strengths which are fairly comparable to concrete cast with regular aggregates (Tay et al, 2002 (Shetty, 1988 Eluozo 2015). It is one of the problems that are characterizing communities in Nigeria which is oil spillage. In fact, it is a major environmental concern in the Niger Delta area. Other areas are not left out as oil spillage occur as a result of pipeline vandalism and inadequate care on oil production operations. Between 1976 and 1996, Nigeria recorded a total of 4,835 oil spill incidents that resulted in a loss of about 1.9 billion barrels of oil to the environment (Badejo & Nwilo, 2004 Eluozo 2013a, 2013b; 2015)

2. GOVERNING EQUATION

$$\theta_w V \frac{\partial c}{\partial t} = \theta_M \frac{\rho_B}{\rho_W} V \frac{\partial^2 c}{\partial x^2} \quad \ldots\ldots\ldots\ldots\ldots\ldots\ldots\ldots\ldots\ldots\ldots\ldots \quad (1)$$

Substituting solution C = ZT into (1), we have

$$\theta_w vZT^1 = \vartheta \frac{\rho_b}{\rho_w} VZ^{11}T \quad \ldots\ldots\ldots\ldots\ldots\ldots\ldots\ldots\ldots\ldots\ldots\ldots \quad (2)$$

$$\vartheta_w \frac{T^1}{T} = -\theta_M \frac{\rho_b}{\rho_w} V \frac{Z^{11}}{Z} T \quad \ldots\ldots\ldots\ldots\ldots\ldots\ldots\ldots\ldots\ldots \quad (3)$$

$$\theta_W \frac{T^1}{T} \quad -\vartheta \frac{\rho_b}{\rho_w} V \left(\frac{Z^{11}}{Z} \right) \quad \ldots\ldots\ldots\ldots\ldots\ldots\ldots\ldots\ldots\ldots \quad (4)$$

$$\vartheta_W V \frac{T^1}{T} \quad -\frac{Z^{11}}{Z} \quad \ldots\ldots\ldots\ldots\ldots\ldots\ldots\ldots\ldots\ldots \quad (5)$$

Considering when Ln x → 0

$$\theta_W V \frac{T^1}{T} = \vartheta_M \frac{\rho_b}{\rho_W} V \frac{Z^{11}}{Z} - T = \lambda^2 \qquad \text{.................................. (6)}$$

$$\theta_W V \frac{T^1}{T} = \lambda^2 \qquad \text{.................................. (7)}$$

$$\frac{Z^{11}}{Z} = \lambda^2 \qquad \text{....................................... (8)}$$

$$\theta_M \frac{\rho_b}{\rho_W} V = \lambda^2 \qquad \text{....................................... (9)}$$

This implies that equation (10) can be expressed as:

$$\theta_M \frac{\rho_b}{\rho_w} v \frac{Z^{11}}{Z} = \lambda^2 \qquad \text{....................................... (10)}$$

$$\theta_M \frac{\rho_b}{\rho_w} V \frac{Z^2}{Z} = \lambda^2 \qquad \text{....................................... (11)}$$

$$\vartheta_W V \frac{dy^2}{dx^2} = \lambda^2 \qquad \text{....................................... (12)}$$

$$\theta \frac{\rho_b}{\rho_w} V \frac{dy^2}{dz^2} = \lambda^2 \qquad \text{....................................... (13)}$$

$$\vartheta_W V \frac{d^2 y}{dz^2} = \lambda^2 \qquad \text{....................................... (14)}$$

$$\frac{d^2 y}{dz^2} = \frac{\lambda^2}{\vartheta_W V} \qquad \text{....................................... (15)}$$

$$d^2 y = \left(\frac{\lambda^2}{\theta_W V}\right) dz^2 \qquad \text{....................................... (16)}$$

$$\int d^2 y = \int \frac{\lambda^2}{\vartheta_W V} dz^2 \qquad \text{....................................... (17)}$$

$$dy = \frac{\lambda^2}{\vartheta_W V} x \, dz \qquad \text{....................................... (18)}$$

$$\int dy = \int \frac{\lambda^2}{\vartheta_W V} Z\,dz + C_1 \quad \ldots\ldots\ldots\ldots\ldots\ldots \quad (19)$$

$$y = \frac{\lambda^2}{\theta_w V} Z + C_1 x + C_2 \quad \ldots\ldots\ldots\ldots\ldots\ldots \quad (20)$$

$$y = \frac{\lambda^2}{\theta_W V} + C_1 x + C_2 \quad \ldots\ldots\ldots\ldots\ldots\ldots \quad (21)$$

$$y = 0$$

$$\Rightarrow \frac{\lambda^2}{\theta_W V} X^2 + C_1 x + C_2 = 0 \quad \ldots\ldots\ldots\ldots\ldots\ldots \quad (22)$$

Applying quadratic expression, we have

$$x = \frac{-b \pm \sqrt{b^2 - 4ac}}{2a} \quad \ldots\ldots\ldots\ldots\ldots\ldots \quad (23)$$

Where a = $\frac{\lambda^2}{\theta_W V}$, b = C_1 and c = C_2

$$X = \frac{-(C_1) \pm \sqrt{(C)^2 - 4\left(\frac{\lambda^2}{\theta_W V}\right) C_2}}{2\frac{\lambda^2}{\theta_W V}} \quad \ldots\ldots\ldots\ldots\ldots\ldots \quad (24)$$

$$= \frac{-C_1 \pm \sqrt{C_1{}^2 - 4C_2 \frac{\lambda^2}{\theta_W V}}}{2\frac{\lambda^2}{\theta_W V}} \quad \ldots\ldots\ldots\ldots\ldots\ldots \quad (25)$$

$$X = \frac{-C_1 + \sqrt{C_1{}^2 - 4C_2 \frac{\lambda^2}{\theta_W V}}}{2\frac{\lambda^2}{\theta_W V}} \quad \ldots\ldots\ldots\ldots\ldots\ldots \quad (26)$$

$$X = \frac{-C_1 + \sqrt{C_1^{\,2} - 4C_2 \dfrac{\lambda^2}{\theta_W V}}}{2\dfrac{\lambda^2}{\vartheta_W V}} \quad \ldots\ldots\ldots\ldots\ldots\ldots\ldots\ldots \quad (27)$$

$$X = \frac{-C - \sqrt{C_1^{\,2} - 4C_2 \dfrac{\lambda^2}{\vartheta_W V}}}{2\dfrac{\lambda^2}{\vartheta_W V}} \quad \ldots\ldots\ldots\ldots\ldots\ldots\ldots\ldots \quad (28)$$

Substituting equation (20) to the following boundary conditions and initial values condition

$$t = 0 \quad C = 0 \quad \ldots\ldots\ldots\ldots\ldots\ldots\ldots\ldots \quad (29)$$

Therefore, $X_{(x)} = C_1 \ell^{-mx} + C_2 \ell^{m_2 x}$ .... (30)

$$C_1 \, Cos \, M_1 x + C_2 \, Sin \, M_2 x \quad \ldots\ldots\ldots\ldots\ldots\ldots\ldots\ldots \quad (31)$$

$$y = \frac{\lambda^2}{\theta_W V} + C_1 + C_2 \quad \ldots\ldots\ldots\ldots\ldots\ldots \quad (32)$$

But if $x = \dfrac{v}{t}$

Therefore, equation (33) can be expressed as:

$$C(x,t) = \left(C_1 \, Cos \, M_1 \frac{\lambda^2}{\theta_W V} \frac{d}{v} + C_2 \, Sin \, M_2 \frac{\lambda^2}{\theta_W V} v.t \right) \quad \ldots\ldots\ldots\ldots\ldots\ldots \quad (33)$$

3. MATERIALS AND METHOD

Standard laboratory experiment where performed to monitor hydrocarbon concentration on concrete pavement, the experimental result are applied to be compared with theoretical values to determined the validation of the model.

4. RESULT AND DISCUSSION

Results and discussion are presented in tables including graphical representation of hydrocarbon concentration

Table:1 Hydrocarbon concentration at different curing age

Curing age	Concentration[Mg/L]
3	84
6	168.77
9	253.15
12	337.54
15	421.92
18	506.31
21	590.04
24	675.08
27	759.47
30	843.56

Table: 2 Hydrocarbon concentration at different curing age

Curing age [Per Day]	Concentration[Mg/L]
10	84
20	168.77
30	253.15
40	337.54
50	421.92
60	506.31
70	590.04
80	675.08
90	759.47
100	843.56

Table: 3 Theoretical and Experimental values for Hydrocarbon Concentration at Different Curing Age

Curing age	Theoretical values [Mg/l]	Experimental values [Mg/L]
3	84	85
6	168.77	166.78
9	253.15	266.23
12	337.54	334.23
15	421.92	444.11
18	506.31	499.87
21	590.04	588.78
24	675.08	689.11
27	759.47	766.45
30	843.56	855.23

Table: 3 Theoretical and Experimental values for Hydrocarbon Concentration at Different Curing Age

Curing age	Theoretical values [Mg/l]	Experimental values [Mg/L]
10	84	85
20	168.77	166.78
30	253.15	266.23
40	337.54	334.23
50	421.92	444.11
60	506.31	499.87
70	590.04	588.78
80	675.08	689.11
90	759.47	766.45
100	843.56	855.23

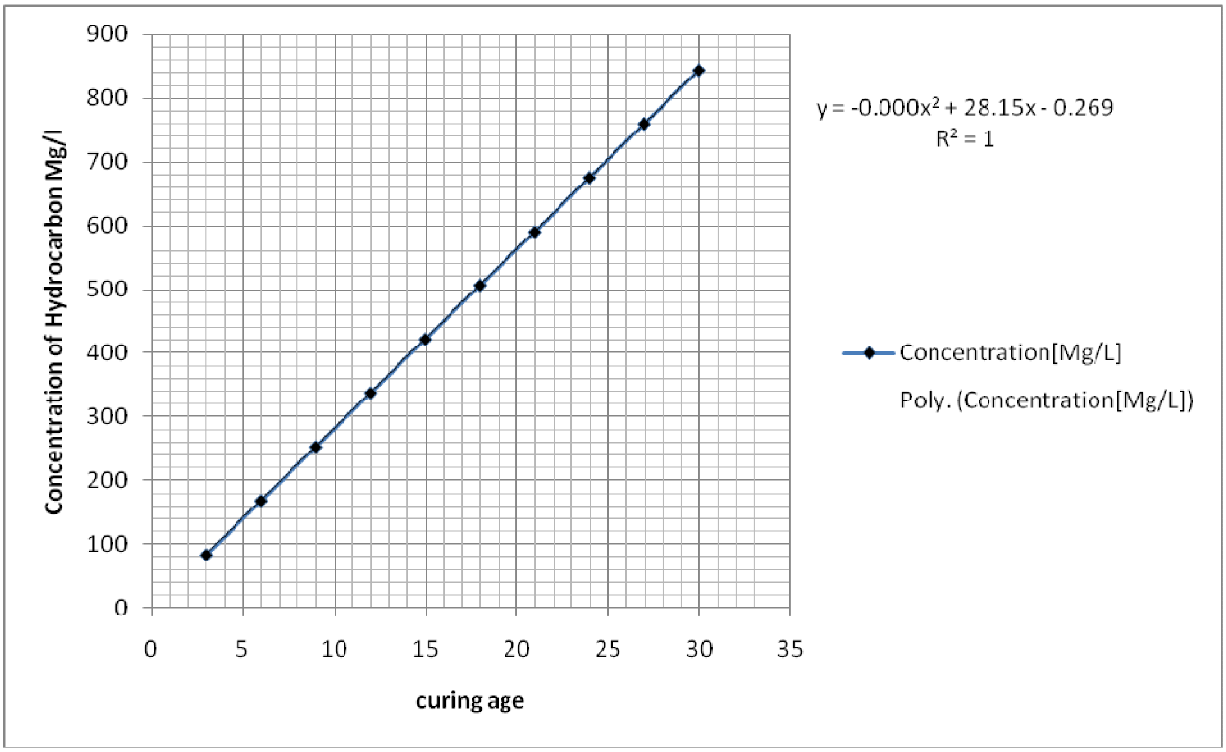

Figure: 1 Hydrocarbon concentration at different curing age

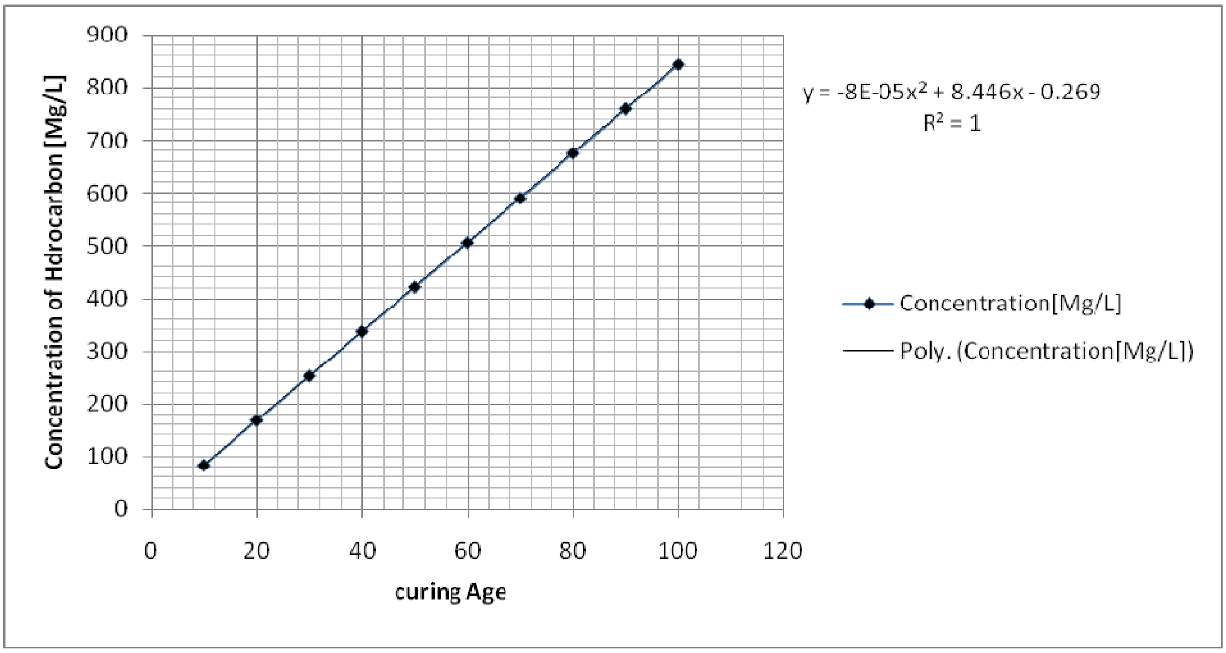

Figure: 2 Hydrocarbon concentration at different curing age

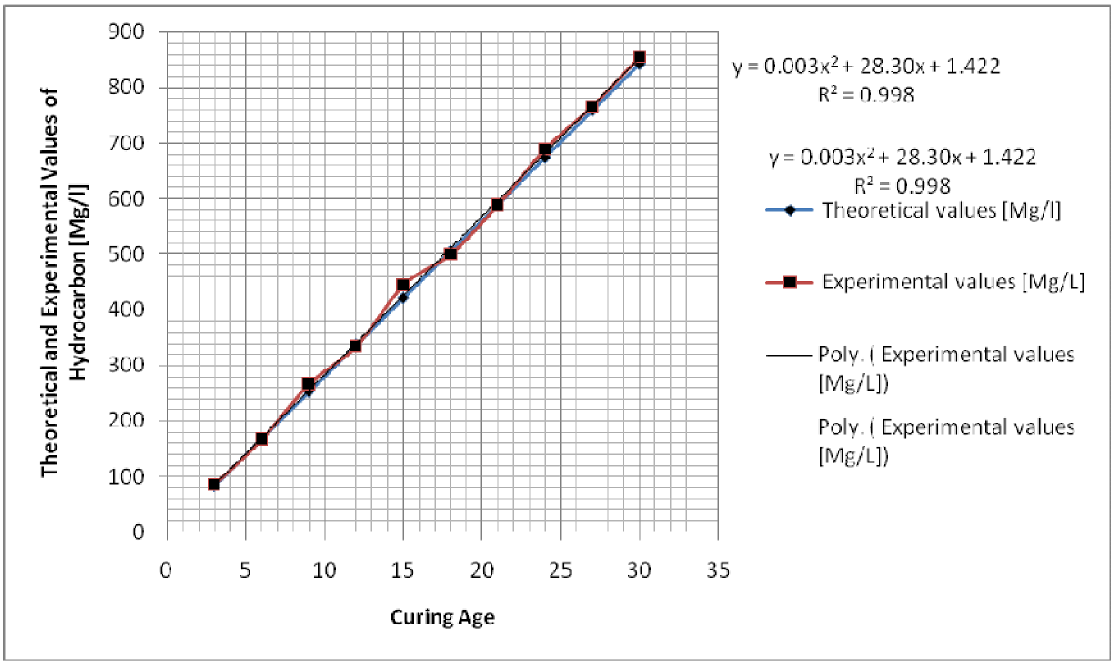

Figure: 3 Theoretical and Experimental values for Hydrocarbon Concentration at Different Curing Age

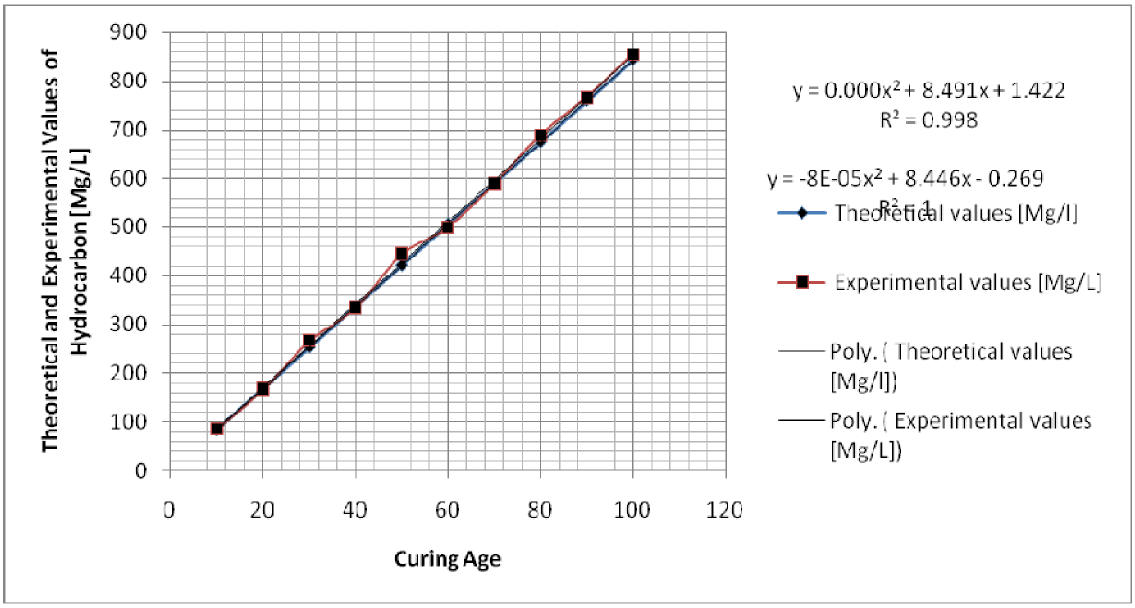

Figure: 4 Theoretical and Experimental values for Hydrocarbon Concentration at Different Curing Age

The expression shows the behavior of the system in terms of concentration level from the concrete contaminated with hydrocarbon. figure one express the results in exponential phase, the concentration were observe increasing to the optimum level recorded at thirty days, similar condition were observed in figure two, the progressive concentration were observed experiences to the optimum rate at hundred curing age, the level of concentration observed were much higher than that of figure one. Figure three observed exponential phase were comparism between the predictive and experimental values was established, both parameters developed faviourable fits linear increase in concentration were observed to the optimum value at thirty days of curing age. Figure four developed similar expression like figure three, progressive increase were experienced in linearized rate to the optimum level, comparism between the predictive and experimental values also expressed best fits, the rate of increase were monitored at different curing age, the concentration were observed increasing to the optimum level, these implies that the concentration were predominant in the concrete formation, the rate of increase experienced are base on the rate of porosity of concrete including permeation on the concrete formation influencing higher rate of concentration, these were experienced in exponential phase to the optimum level, these expression are reflected on the compressive strength of the concrete pavement.

4. CONCLUSION

Inducing of hydrocarbon on concrete pavement has been express in various dimensions, the study were expressed through developed mathematical derived model, the simulation was to monitor the rate of concentration of hydrocarbon induced in concrete pavement , the rate of concentration predominantly in linear exponential phase has expressed the rate of high porosity in the concrete pavement. Such condition has expose lower deposition of compressive strength in the system, the derived model simulation values were compared with experimental results, both parameters developed faviourable fits, the expression of concrete pavement with high induced hydrocarbon has shows high rate of hydrocarbon deformation in concrete pavement, the study is imperative because it has express the rate of hydrocarbon induce in concrete formation, these are base on the type of mix design and rate of porosity and permeability, the rate decrease in compression will be very high if it is monitored.

5. REFERENCES

[1] Gbenga Matthew Ayininuola Influence of diesel oil and bitumen on compressive strength of concrete Journal of Civil Engineering (IEB), 37(1) (2009) 65-71

[2] Al-Mutairi, N. M. (1995). "Kuwait Oil-based Pollution: Effect on building material", Journal of Materials in Civil

Engineering ASCE, Reston; 7 (3), 154 – 160.

[3] Shetty, M. S. (1988). Concrete technology theory and practice, 3rd ed. S. Chand and company limited, New Delhi, India.

[4] Tay, J. H., Show, K. Y. and Hong, S. Y. (2002). Concrete aggregates made from sludge-marine clay mixes, Journal of materials in civil engineering, ASCE, Reston; 14 (5), 392 – 398.

[5] Wilson, S. A,, Langdon, N. J. and Walden, P. J. (2001). The effects of hydrocarbon contamination on concrete strength, Proceedings Institution of Civil Engineers Geotechnical Engineering, Thomas Telfords, London, 189 – 193

[6] Badejo, O. T. and Nwilo, P. C. (2004). Manage ment of oil spill dispersal along the Nigerian coastal areas, Department of Surveying and Geoinformatics, University of Lagos, Lagos.

[7] Blaszczynski, T. and Scigallo, J. (2006). "Assessment of ultimate bearing capacity of RC sections affected by mineral oil", Archives of Civil and Mechanical Engineering, Polish Academy of Science, Wroclaw; 6 (2), 41– 56.

[8] Calabrese, E. J., Kostecki, P. T. and Bonazo untas, M. (1991). Hydrocarbon contaminated soils, CRC Press, Taylor and Francis group, Taiwan, Vol. I

[9] Munoz, J. F., Tejedor, I., Anderson, M. A. and Cramer, S. M. (2005). Effect of coarse aggregate clay-coatings on concrete performance, Innovative Pavement Research Foundation Research Report

[10]. Eluozo S.N. 2013 Development of mathematical model to monitor the influences of permeability and porosity in mass concrete formation international journal of materials, methods and technologies vol. 1, no. 8, September 2013, pp:126 -132

[11]. Eluozo S.N. 2013 Predictive model to monitor the rate of diffusion chloride ions transport in homogenous concrete structure world journal of science and technology research vol. 1, no. 4, June 2013, pp: 67

[12]. Eluozo S.N. 2013 Predictive model to monitor the effective rate of alkali silica reaction on pore distribution of aggregate in concrete pavement World Journal of Chemical Science and Engineering Research Vol. 1, No. 1.